Supplementary material

Boundary conditions and numerical solution of Equation 4

The travelling-wave solution for peeling-by-bending is given by $h(x,t) = h_0 F[\xi \equiv (x - ct)/L_p]$, where

$$F^3 F^{(v)} + F = 1. \tag{S1}$$

We have already used the matching condition $h \to h_0$ ($F \to 1$) ahead of the peeling wave to determine the constant of integration when integrating (4) once. We now explain how the matching conditions determine a unique numerical solution to (S1) and thence determine the spreading law (5).

By writing $F = 1 + \phi$, where $\phi \to 0$ as $\xi \to \infty$, we obtain the asymptotic behaviour $\phi^{(v)} + \phi \sim 0$, which has five exponential solutions of the form $\phi \propto \exp(\omega_i \xi)$ with $\omega_i^5 = -1$. Two of the five complex roots ω_i have positive real part, and give growing exponentials. If $F \to 1$, the coefficients of the growing exponentials must be zero, which provides two boundary conditions for (S1).

As $\xi \to -\infty$, we must match to the interior solution (3), where $h \gg h_0$ and so $F \gg 1$. The generic solution of $F^{(v)} = O(F^{-2})$ is a quartic polynomial in ξ. To match to the quadratic behaviour of the interior solution near its edge, we must eliminate the cubic and quartic terms by imposing two further boundary conditions $F''', F'''' \to 0$ as $\xi \to \infty$.

The fifth boundary condition on (S1) corresponds to an arbitrary choice of origin for the coordinate ξ, for example $\xi = 0$ at the first position where $F = 1$, and has no physical significance. With five boundary conditions, we can obtain a unique solution to (S1) numerically and find $F'' \to 1.35$ as $\xi \to -\infty$. The dimensional matching condition $h_0 F''/L_p^2 \to \kappa$ then determines the wave speed c in terms of the curvature κ of the interior solution and the other parameters.

Non-existence of advancing contact-line solutions to Equation 1

In the main text we noted that there are no solutions to (1) with $h = 0$ at an advancing contact line $r = R(t)$ (with $dR/dt > 0$). An informal indication of this result is that the rate of spread dR/dt in (5) tends to zero as the pre-wetting film thickness h_0 tends to zero. More formally, we follow the proof in [1] and suppose that (1) has a solution with a propagating contact line with an asymptotic travelling-wave behaviour $h(x,t) \sim A(t)[R(t) - r]^\alpha$ as $r \to R_-(t)$, where $A, \alpha > 0$, and $h = 0$ for $r \geqslant R(t)$. If $B \neq 0$ then the elastic term in (1) dominates the gravitational term as $r \to R$ and the dominant asymptotic balance (i.e. the leading powers of $R - r$) is

$$\frac{dR}{dt} A\alpha(R-r)^{\alpha-1} \sim \frac{B}{12\mu} A^4 \alpha(\alpha-1)(\alpha-2)(\alpha-3)(\alpha-4)(4\alpha-5)(R-r)^{4\alpha-6}. \tag{S2}$$

By equating the exponents of $R - r$, we obtain $\alpha = 5/3$, and by equating the coefficients, we deduce

$$\frac{dR}{dt} = -\frac{280}{243}\frac{B}{12\mu} A^3. \tag{S3}$$

We conclude that (1) can only have solutions with a *retreating* contact line ($dR/dt < 0$), but not with an advancing contact line ($dR/dt > 0$). This conclusion is in agreement with detailed mathematical analysis [1] of the equation $h_t = (h^n h_{xxxxx})_x$, which only has advancing contact-line solutions for $n < 5/2$ and has only retreating solutions for $n = 3$ (and even these are underspecified and require external forcing of the rate of retreat). Both

[2] and [3] appeal to advancing contact-line solutions: we believe the peeling front was not numerically resolved in [2], and we note that equation (11) of [3] has a sign error, which originates in a sign error in the transformation to moving coordinates in equation (7).

The non-existence of advancing contact-line solutions to (1) parallels the well-known non-existence of advancing contact-line solutions to the analogous equation for surface-tension driven spreading [4, 5]

$$\frac{\partial h}{\partial t} = -\frac{\gamma}{3\mu}\boldsymbol{\nabla}\cdot(h^3\boldsymbol{\nabla}\nabla^2 h). \tag{S4}$$

Analysis of (S4) with a pre-wetting layer instead of a contact line leads to the Landau–Levich differential equation $F^3F''' = F - 1$, which is directly analogous to the elastic peeling-wave equation (S1).

In a different situation where there is no pre-wetting fluid layer then the lack of advancing contact-line solutions to (1) shows that some other physical process must be invoked at the front if propagation is to occur. For example, [6] and [7] consider the case where the front is controlled by brittle fracture and find that R scales as $t^{1/4}$ and then $t^{1/2}$.

Image analysis

Deformation of the elastic (PDMS) sheet was imaged by a Nikon digital SLR camera (D5000) with a resolution of 4288×2848 pixels by tracking the deflection of a line drawn on the surface. At the working distances typically used this resolution implies a spatial resolution of 5-7 pixels per millimetre ($150 - 200\,\mu$m per pixel). The precise value of the spatial scaling was determined for each experiment by calibrating against a 500 millimetre long ruler. For optimal contrast, the line is fluorescent, illuminated by a blue light, and a red filter placed on the camera. A raw image taken using the technique is reproduced in figure 1 and shows the excellent contrast achieved.

FIG. 1. Sample raw image of deflected line.

Deflections of the line are imaged by subtracting the current position of the line from a reference, undeflected, image. The physical width of the fluorescent line is approximately 1.5 ± 0.3 mm, and varies across the image. Sub-pixel resolution can be obtained by locally fitting the intensity of the deflected and reference lines, and using the information in the shape of the intensity curve. For example, in supplementary figure 2 we show how a fitted Gaussian profile of image intensity across the fluorescent line determines the location of the central peak to sub-pixel accuracy at one location. The scatter among neighbouring locations is similar to the statistical uncertainty in the fit at one location. In the inset of figure 2 (main text), this scatter is reduced by taking a 20-point running average. Note that, by always subtracting the deflected image from the reference, any irregularities in the line itself (e.g. variations due to non-uniform line width) are automatically accounted for in the image analysis.

The elastic sheet was reflectively smooth, and its thickness was measured at several points with a micrometer.

[1] J. C. Flitton and J. R. King, Euro. J. Appl. Math. **15**, 713 (2004).

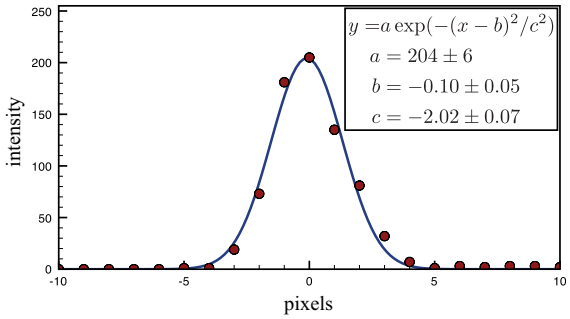

FIG. 2. Sample image intensity across the imaged line, along with a Gaussian fit. The statistical uncertainty in the position of the Gaussian peak is 0.05 pixels, corresponding to about 10 μm.

[2] C. Michaut, J. Geophys. Res. **116**, B05205 (2011).
[3] T. T. Al-Housseiny, I. C. Christov, and H. A. Stone, Phys. Rev. Lett. **111**, 034502 (2013).
[4] C. Huh and L. E. Scriven, J. Colloid Interface Sci. **35**, 85 (1971).
[5] J. R. King and M. Bowen, Euro. J. Appl. Math. **12**, 321 (2001).
[6] A. P. Bunger and E. Detournay, Engng. Fract. Mech. **72**, 2468 (2005).
[7] A. P. Bunger and A. R. Cruden, J. Geophys. Res. **116**, B02203 (2011).